Published in final edited form as:
Mol Cancer Res. 2013 March ; 11(3): 303–312. doi:10.1158/1541-7786.MCR-12-0478.

Acquisition of the metastatic phenotype is accompanied by H_2O_2-dependent activation of the p130Cas signaling complex

Nadine Hempel[1], **Toni R. Bartling**[1], **Badar Mian**[2], and **J. Andres Melendez**[1]

[1]College of Nanoscale Sciences and Engineering, University at Albany, SUNY, Albany, NY 12203, U.S.A

[2]Stratton VA Medical Center and Albany Medical Center, Albany, NY 12208, U.S.A

Abstract

Reactive Oxygen Species (ROS) have emerged as cellular signaling molecules and are implicated in metastatic disease by their ability to drive invasion and migration. Here we define the signaling adaptor protein p130Cas as a key redox-responsive molecular trigger that is engaged in highly invasive metastatic bladder tumor cell lines. Endogenous shifts in steady-state H_2O_2 that accompany the metastatic phenotype increase p130Cas phosphorylation, membrane recruitment and association with the scaffolding protein-Crk and subsequent Rac1 activation and actin reorganization. Both enzymatic and non-enzymatic scavenging of H_2O_2 abrogates p130Cas-dependent signaling and the migratory and invasive activity of the metastatic bladder tumor cells. Disruption of p130Cas attenuates both invasion and migration of the metastatic variant (253J-BV). 253J-BV cells displayed an increase in global thiol oxidation and a concomitant decrease in total phosphatase activity, common target proteins of active-site cysteine oxidation. The dependence of phosphatases on regulation of p130Cas was highlighted when depletion of PTPN12 enhanced p130cas phosphorylation and the migratory behavior of a non-invasive parental bladder tumor control (253J). These data demonstrate that the metastatic phenotype is accompanied by increases in steady-state H_2O_2 production that drive pro-migratory signaling and suggest that antioxidant-based therapeutics may prove useful in limiting bladder tumor invasiveness.

Keywords

reactive oxygen species; redox signaling; metastasis; hydrogen peroxide; PTPN12; PTP-PEST

INTRODUCTION

The ability of a tumor cell to invade and migrate through the basement membrane and extracellular matrix (ECM) is a vital first step in tumor metastasis. Tumor cell invasion is accompanied by protease driven ECM degradation and reorganization of cellular signaling components at the leading and lagging edges of the cell, ultimately leading to restructuring of the actin cytoskeleton and migration. An important signaling cascade involved in this process is the Focal Adhesion Kinase (FAK) pathway. Initiation of this cascade involves phosphorylation and engagement of the kinases FAK and Src, leading to recruitment of

To whom correspondence should be addressed: J. Andres Melendez, College of Nanoscale Sciences and, Engineering, University at Albany, SUNY, 257 Fuller Rd., NFE-4313, Albany, NY 12203, USA, Ph: (518) 956-7360, Fax: (518) 437-8687, jmelendez@albany.edu or Nadine Hempel, College of Nanoscale Sciences and Engineering, University at Albany, SUNY, 257 Fuller Rd., NFE-4413, Albany, NY 12203, USA, Ph: (518) 956-7309, Fax: (518) 437-8687, nhempel@albany.edu;.

We wish to confirm that there are no known conflicts of interest associated with this publication and there has been no significant financial support for this work that could have influenced its outcome.

adaptor proteins such as p130cas and Crk to the focal contacts at the leading edge. This complex engages DOC180, a Guanine Nucleotide exchange factor, to activate Rac-1 and consequential actin rearrangement.

Reactive Oxygen Species (ROS) are known DNA damaging agents involved in carcinogenesis. However, at sub-lethal levels, ROS are implicated in regulating a multitude of cellular signaling cascades, primarily due to their ability to reversibly oxidize thiolate anions of cysteine residues [1, 2]. Endogenous ROS are often elevated in cancer cells and this is accompanied by alterations in the cells' antioxidant scavenging potential [3–5]. Thus, cancer cells have uniquely acquired the ability to survive and even thrive despite this chronic, sub-lethal oxidant challenge.

Intracellular ROS production has been linked to metastatic disease progression [6]. The loss of mitochondrial genome integrity is accompanied by an increase in ROS levels that enhance the metastatic potential of tumor cells [7]. ROS of both mitochondrial and non-mitochondrial origin are associated with regulating cellular signaling pathways, which are implicated in metastatic disease [2, 8]. We have demonstrated that enhanced invasion and migration are associated with intrinsic increases in the intracellular H_2O_2 milieu and changes in antioxidant expression, using a model of metastatic bladder cancer progression [9, 10]. This represents a patho-physiologically relevant model that does not rely on manipulation of mitochondrial genome integrity [7], NADPH oxidase stimulation, following receptor or integrin engagement [6], nor manipulating antioxidant expression [11, 12] to change intracellular redox status. Two-fold picomolar increases in intracellular H_2O_2 (18→32 pM) in the metastatic bladder cancer cell variant 253J-BV are associated with enhanced MMP-9 and VEGF expression and increased clonogenicity compared to the related parental cells 253J [9, 10]. Here we set out to test the hypothesis that metastatic cancer cells have uniquely adapted to thrive with an enhanced intracellular ROS milieu and evolved to utilize oxidation as a novel mechanism to drive pro-migratory signaling events by H_2O_2-dependent activation of the p130Cas signaling complex.

MATERIALS AND METHODS

Cell Culture, treatments and transfection

253J and 253J-BV cells were created and cultured as described previously [9, 10]. Cells were treated with H_2O_2 (Sigma-Aldrich, St. Louis, MO, USA) in serum-free DMEM. Cells were pretreated in DMEM +10%FBS with either 500U/ml bovine CAT (Sigma-Aldrich) or 2mM N-acetyl-L-cysteine (NAC; Sigma-Aldrich) for 18–24 hours, followed by the same treatments in serum-free media for the duration of the experiments, as indicated. Alternatively, CAT or control beta galactosidase (Lac-Z; MOI 100) were expressed using adenoviral gene delivery [10]. CAT activity was determined as described previously [10].

The following siRNA constructs were transfected into 200,000 cells using RNAi Max Lipofectamine reagent (Invitrogen-Life Technologies, Carlsbad, CA, USA): 200pmol PTPN12 Silencer Select siRNA (Ambion), 100pmol p130Cas siRNA (Santa Cruz Biotechnology, Santa Cruz, CA, USA) or equal molar concentration of Non-Targeting siRNA (control #1, Dharmacon-Thermo Scientific, Lafayette, CO).

Wound Healing and Matrigel Invasion Assays

Wound Healing and Matrigel Invasion Assays were essentially carried out as previously described [12]. For Matrigel transwell (BD Biosciences, San Jose, CA, USA) experiments 25,000 253J-BV cells were applied to the top of the chamber, with indicated treatments, and allowed to invade (24hrs) towards 10% serum DMEM as the chemo-attractant. Cells invading to the underside of the filter were fixed, stained (0.8% NaCl, 50% ethanol, 5%

formaldehyde, 0.2% crystal violet) and quantified. Images of wounds and matrigel filters were obtained using a Zeiss Axio Observer.Z1 with an EC Plan-Neofluar 5x/0.15 M27 objective and AxiocamMR3. No appreciable invasion through Matrigel could be observed with 253J cells with the same assay conditions.

MMP-1 semi-quantitative real-time RT-PCR

Following RNA isolation (TRizol, Life Technologies) and reverse transcription (Superscript II, Life Technologies) real time semi-quantitative RT-PCR was carried out on an Applied Biosystems 7500 Real Time PCR cycler, using SYBR green and the following primers: MMP-1 sense 5′-AGT GAC TGG GAA ACC AGA TGC TGA-3′, MMP-1 antisense 5′-GCT CTT GGC AAA TCT GGC GTG TAA-3′; Actin sense 5′-ACC AAC TGG GAC GAC ATG GAG-3′, Actin antisense 5′-TAG CAC AGC CTG GAT AGC AAC GTA-3′. Data were analyzed using the comparative CT method with values normalized to β-Actin levels and expressed relative to MMP-1 expression in 253J cells.

Antibodies, Immunoblotting and Immunoprecipitation

The following antibodies were used in the study: Crk, p130Cas, Anti FITC (BD Biosciences), Phospho p130Cas Y165, Fak Y397, Src, Src Y416 (Cell Signaling), PTP-PEST, EGF-R (Santa Cruz Biotechnology), PTPN12, CAT, PY20 phospho tyrosine (Abcam, Cambridge, MA, USA), GAPDH (Ambion-Life Technologies). Cells were lyzed using RIPA buffer (150mM NaCl, 50mM Tris pH 7.5, 1% NP-40, 0.5% deoxycholate, protease inhibitor cocktail [Roche], 1mM sodium orthovanadate). Cleared lysates were quantified for protein concentration (BCA, Thermo Scientific) and loaded on either 4–12% NuPAGE (Life Technologies) or 10% SDS-PAGE. For immunoprecipitation, protein (1mg) was incubated with anti-Crk antibody (1μg) and protein G sepharose, and eluded in 2x reducing SDS-PAGE buffer. Following electrophoresis, transfer to nitrocellulose membrane (iBlot, Life Technologies) and blocking, primary antibody incubation was carried out in 5% BSA TBS-0.1%Tween (1:1000). Secondary HRP-conjugated mouse or rabbit antibodies (GE Healthcare, Pittsburgh, PA, USA) at 1:10,000 dilutions were added followed by chemiluminescence detection (Pico & Femto ECL reagents, Thermo Scientific).

Membrane/cytoskeletal fractionation

The membrane/cytoskeletal fractions were obtained using a protocol adapted from Zhao *et al.* [13]. Cells were lyzed in CSK buffer (0.5% Triton X-100, 10mM TrisHCl (pH 6.8), 50mM NaCl, 300mM sucrose, 3mM $MgCl_2$, 1mM sodium orthovanadate and protease inhibitors) at 4°C. Following centrifugation (13,600g, 30min, 4°C), the supernatant, Triton X soluble cytosolic fraction was removed and analyzed for protein content. The triton X insoluble pellet (membrane/cytoskeletal fraction) was washed, resuspended in SDS buffer (1% SDS, 10mM TrisHCl (pH 7.5), 2mM EDTA, 1mM sodium orthovanadate and protease inhibitors) and boiled. The supernatant Triton X insoluble fraction was cleared from cell debris by centrifugation (13,600g, 30min 4°C). Equivalent amounts of triton X insoluble fraction in reference to soluble fraction protein concentration were electrophoresed, followed by immunoblotting.

Immunofluorescence Staining

Cells grown on glass coverslips were fixed with 4% paraformaldehyde/PBS, permeabilized (0.1% TritonX100/PBS) and blocked (3% FBS/PBS). Incubation with phospho-p130Cas Y165 antibody (1:100) was followed by anti rabbit Alexa-Fluor 488 conjugated antibody (Life Technologies, 1:1000). F-actin was stained with Phaloidin Texas-Red (Life Technologies, 1:50) and nuclear DNA with Dapi. Cells were mounted (Prolong Gold Antifade, Life Technologies) and images taken on a Zeiss Axio Observer.Z1Fluorescence

Microscope (HBO100 illuminator), using an EC Plan-Neofluar 63× 1.25 NA, oil immersion objective and AxioCam MR3 with Apotome attachment. Image analysis was performed using Axiovision software (Zeiss). Alternatively, images were acquired using an Olympus Fluoview 1000 Confocal Microscope with a UPLSAPO 60×/1.2 NA water immersion objective and analyzed using Fluoview software (Olympus). Subsequent processing was undertaken using Image J or Adobe Photoshop to uniformly change size, brightness and contrast of the entire image.

Rac1 Activation Assay

Active GTP-bound Rac1 was precipitated from lysates using the p21 binding domain (PBD) of p21-activated protein kinase (PAK1) bound to agarose beads. The Rac1/Cdc42 Activation Assay was purchased from Millipore and carried out as per manufacturer's instructions.

Iodoacetamide labeling of disulfides and reduced cysteines

In Situ reverse 5-iodoacetamidofluoresceine (5-IAF) labeling was adapted from Yang *et al.* [14]. Following H_2O_2 treatment cells were fixed in methanol and permeabilized (TritonX100). Free/reduced cysteines were blocked with 200mM iodoacetic acid (IAA; Sigma-Aldrich) in 100mM Tris (pH8.3), 5mM EDTA (37°C, 1hr). Following washes (TBS/EDTA), oxidized thiols were reduced with 1mM DTT, 100mM Tris (pH8.3), 5mM EDTA (30min, room temperature), with IAA alkylated residues being protected from this reduction step. Re-reduced thiols were subsequently labeled with 1mM 5-IAF (Life Technologies) in 100mM Tris (pH8.3), 5mM EDTA (30min, room temperature) and cells mounted (Prolong). Images were taken as described above, background corrected and fluorescence intensity quantified using Fluoview software.

Protein Phosphatase Activity Assay

Total phosphatase activity of cellular lysates was assessed using cholorimetric analysis of dephosphorylation of para-nitrophenol phosphate (pNPP, Thermo Scientific) according to Streit *et al.* [15].

Statistical Analysis

All figures are representative of at least three replicate experiments. Data are presented as mean +/− standard error of the mean (SEM). T-tests and one-way ANOVA with Tukey's Multiple Comparison Post-tests were performed using Prism 5.01 (GraphPad Software, La Jolla, CA, USA).

RESULTS

Intracellular increases in ROS contribute to enhanced migration and invasion of metastatic bladder cancer cells

The highly metastatic 253J-BV cell line was derived from a poorly metastatic parental human bladder carcinoma cell line, 253J, following five successive bladder xenografts [9]. We previously demonstrated that 253J-BV cells display a nearly 2-fold increase in intracellular steady-state H_2O_2 compared to 253J cells (18→32 pM) [10]. 253J-BV cells also exhibit an altered antioxidant profile, with increased Sod2 expression, decreased catalase (CAT) expression, and a decrease in reduced to oxidized glutathione ratio (GSH/GSSG) [10]. We next asked whether the metastatic 253J-BV cell line displays increases in its *in vitro* migratory and invasive behavior. Utilizing a classical scratch-wound assay to measure basic cell migration parameters the metastatic 253J-BV variant exhibited enhanced migration *in vitro* when compared to the parental 253J line (Fig. 1A). Similarly, using matrigel-coated transwell assays to assess invasion, only the 253J-BV cells were able to

invade through the matrigel matrix. Addition of the H_2O_2 –detoxifying enzyme catalase (CAT) or the antioxidant N-acetyl-L-cysteine (NAC) significantly attenuated the migratory capacity of 253J-BV cells (Fig. 1B). 253J-BV cell invasion was also impaired by CAT and NAC treatments (Fig. 1C). Treatment of both cells with low dose H_2O_2 (5–50μM) stimulated migration (Fig. 1D). This low dose H_2O_2 treatment did not result in cytotoxicity to either cell line. Interestingly, the basal migration rate of 253J cells was not significantly altered by CAT or NAC treatment (Suppl. Fig. 1). These data implicate ROS as participants in regulating the migratory and invasive behavior of the metastatic 253J-BV cells.

Redox dependent p130Cas phosphorylation regulates focal adhesion kinase (FAK) signaling

Due to the important contribution of ROS in cellular signaling we monitored whether shifts in steady-state H_2O_2 augment pro-metastatic signaling networks within 253J-BV cells. We first evaluated the phosphorylation state of Focal adhesion kinase (FAK), as it plays an important role in cancer cell migration and is redox-responsive [16–19]. We found that both total FAK and its (Y397) phosphorylation were moderately elevated in 253J-BV cells and this was attenuated by CAT treatment (Fig. 2A). FAK^{Y397} creates a binding site for Src kinase whose (Y416) phosphorylation state remained constant between the two cell lines. Interestingly, total Src levels were diminished in 253J-BV lysates relative to the 253J parental cells, and may reflect a depletion of its cytosolic pools. This finding may suggest that Src^{Y416} predominates in the metastatic variant which in turn facilitates FAK-Src signaling. Interestingly, Src phosphorylation remained unchanged following CAT treatment (Fig. 2A).

Active FAK-Src facilitates p130Cas (Crk-associated substrate) binding and phosphorylation. The adaptor protein p130Cas links FAK-Src to DOC180, enabling this Guanine Nucleotide exchange factor to activate Rac-1. Phosphorylation of p130Cas (Y165) was robustly enhanced in 253J-BV cells (4.2 fold ± 0.7 compared to 253J) and this increase was attenuated by 68% following treatment with exogenous CAT (Fig. 2A) or by adenoviral-mediated CAT expression (Fig. 2B), indicating that phospho-p130Cas status is H_2O_2-dependent. Conversely, p130Cas phosphorylation was increased in non-metastatic 253J cells following treatment with low dose H_2O_2 (Fig. 2C). The effect of exogenous H_2O_2 treatment was less evident in 253J-BV cells, presumably due to the high endogenous phospho-status of p130Cas in the metastatic cells.

Intracellular redox status regulates membrane localization of p130Cas

Phosphorylation of p130Cas is necessary for its membrane recruitment to focal contacts in migrating cells [20, 21]. Cellular fractionation revealed that total and phosphorylated $p130Cas^{Y165}$ levels were significantly higher in membrane fractions from 253J-BV cells under control conditions compared to the parental line (Fig. 3A & 3B). Membrane association of both p130Cas and $p130Cas^{Y165}$ were significantly enhanced in non-metastatic 253J cells following treatment with increasing concentrations of H_2O_2 (Fig. 3A & 3B; see Suppl. Fig. 2 for fractionation controls). Phosphorylation occurred rapidly and was observed as early as 10 minutes post H_2O_2 treatment. Further, 253J-BV cells displayed enhanced $p130Cas^{Y165}$ localization to membrane protrusions, as assessed by immunofluorescence. Equivalent analysis of the non-metastatic 253J cells revealed a distinct uniform cellular distribution of $p130Cas^{Y165}$ (Fig. 3C). In addition, 253J-BV cells exhibited differential actin cytoskeletal distribution, with enhanced accumulation of actin fibers at the cell periphery.

The localization p130Cas was also strongly enhanced in filopodia-like protrusions of metastatic cells. In the scratch-wound assay the frequency of $p130Cas^{Y165}$ positive protrusions at the leading edge of 253J-BV cells was quantified and shown to be

significantly higher than in 253J cells (Fig. 3D, F, H). Treatment of 253J cells with 50μM H_2O_2 significantly increased the number of positive protrusions for $p130Cas^{Y165}$ (Fig. 3D, E & H). Conversely, CAT treatment drastically reduced $p130Cas^{Y165}$ positive protrusions in 253J-BV cells (Fig. 3F, G & H). These data suggest that the increases in $p130Cas^{Y165}$ in 253J-BV cells, relative to 253J cells, are in large part redox-dependent and likely contribute to the redistribution of F-actin in membrane protrusions of metastatic cells.

Cellular redox state influences p130Cas mediated downstream signaling

Following phosphorylation and membrane localization p130Cas associates with Crk to initiate GTPase recruitment and downstream signaling. Analysis of Crk-associated p130Cas using co-immunoprecipitation revealed a marked increase in p130Casbound Crk in the metastatic 253J-BV cells that was attenuated by CAT treatment (Fig. 4A). Further, the amount of active GTP-bound Rac-1 was decreased in the 253J-BV cells, following both adenoviral CAT expression and treatment with exogenous CAT (Fig. 4B). These findings indicate that p130Cas association with Crk is under redox-control and likely participates in the robust migratory signaling activity of the metastatic 253J-BV cells. To directly assess the role of p130Cas in migratory signaling, we silenced its expression in both the 253J and 253J-BV cells and observed a significant decrease in the migratory behavior of both cell lines as compared to control siRNA treated cells (Fig. 4C). The impact of p130Cas suppression on 253J-BV invasion was more pronounced, displaying a near complete inhibition of invasion (Fig. 4D). The non-metastatic 253J cells display no invasive activity thus the impact on p130Cas suppression using this assay was not assessed. These findings clearly establish the important contribution of p130Cas to the invasive activity of the metastatic 253J-BV bladder cell line.

Redox status of metastatic bladder cancer cells influences global protein thiol disulfide formation and protein tyrosine phosphatase inactivation

ROS play an important role as second messengers in cellular signaling through reversible, oxidative inactivation of regulatory phosphatases [22]. Protein tyrosine phosphatases (PTP) contain active site cysteines, which are susceptible to thiol oxidation due to their low pKa. This oxidation can lead to a number of reversible modifications, such as sulfenic acid and disulfide formation. Thus, oxidative phosphatase inactivation is commonly linked to increases in kinase activity. We hypothesized that increases in steady state H_2O_2 in the 253J-BV cells might result in a global shift in thiol oxidation and a concomitant decrease in phosphatase activity. To monitor global thiol oxidation we used an *in situ* reverse labeling assay. Reduced thiols were first alkylated with iodoacetic acid (IAA) while oxidized residues are protected from this alkylation. Cells are then treated with a strong reductant to reduce all oxidized thiols. The newly reduced non-alkylated thiols are subsequently labeled with fluorescently-tagged 5-iodoacetamide (5-IAF). 253J-BV cells display an increase in 5-IAF labeling relative to the 253J cells, indicating a general increase in thiol oxidation formation (Fig. 5A) which was further enhanced by H_2O_2 treatment. Increased thiol oxidation was also accompanied by a global decrease in phosphatase activity of the 253J-BV cells, that was exacerbated by sub-lethal H_2O_2 treatment (Fig. 5B). These findings suggest that oxidative inactivation of phosphatases may contribute to the enhanced migratory signaling activity of metastatic 253J-BV cells.

The primary phosphatase responsible for regulation of p130Cas phosphorylation is PTPN12 [23]. The importance of PTPN12 in regulating p130Cas phosphorylation and migration was demonstrated when expression of PTPN12 was decreased in the non-metastatic 253J cells. A ~25% knockdown of PTPN12 dramatically increased the level of p130Cas phosphorylation in 253J cells (Fig. 5D). This moderate knockdown resulted in statistically significant increases in 253J cell migration (Fig. 5D). These data indicate that decreases in PTPN12

activity either by oxidation or direct suppression can dramatically influence migratory signaling by maintaining p130Cas^{Y165}.

DISCUSSION

In the present study we demonstrate that subtle increases in steady-state H_2O_2 levels within metastatic bladder cancer cells are sufficient and necessary to drive pro-migratory signaling *via* regulation of p130Cas. These changes are all reliant on subtle picomolar increases in endogenous H_2O_2 levels within the metastatic variant cells (i.e. 253J: 18pM; 253J-BV: 32 pM) without prior treatment or stimulation of cells [10]. We also show that intracellular shifts in steady state H_2O_2 production result in detectable changes in pro-migratory signaling and further shed light on a redox-signaling network that may play an important role in metastatic disease progression.

The role of intracellular H_2O_2 was validated in all cell lines when co-expression or treatment with recombinant CAT effectively abrogated these pro-metastatic phenotypes and signaling cascades [12, 24]. These data also suggest that antioxidant enzyme expression can have profound effects on pro-migratory cellular signaling pathways. Of note are markedly lower basal CAT expression levels previously reported in 253J-BV cells when compared to their parental control [10], which likely explains some of the robust H_2O_2-dependent signaling observed in these cells. It is interesting to note that changes in antioxidant expression profile correlate with metastatic disease. Increased Sod2 levels are commonly associated with more invasive disease and poor patient outcome in a number of cancer types and are constitutively high in 253J-BV cells [5, 10, 25–27]. Elevated Sod2 levels can increase steady state H_2O_2 levels. In addition, recombinant Sod2 expression in 253J cells can significantly increase their invasive potential through matrigel, an effect that is abrogated following CAT co-expression [12]. Further, analysis of microarray data suggests that increasing stage and grade of human bladder cancer is associated with enhanced Sod2 and decreased CAT expression [5, 10]. The factors responsible for driving this differential expression of Sod2 and catalase in these two cell lines is unknown. Nuclear factor erythroid 2-related factor (Nrf-2) is a known regulator of both Sod2 and catalase gene transcription, and nuclear factor kappa B (NF-κB) is a critical player in Sod2 expression. It is interesting to note that in studies using Nrf-2 null mice, Nrf-2 has been shown to be necessary for induction of catalase expression [28], while there is evidence that it negatively regulates Sod2 transcription [29, 30]. Shifts in steady-state H_2O_2 could alter the activation of these important redox-sensitive regulators, and help explain the changes in antioxidant enzyme expression that accompany the metastatic phenotype.

H_2O_2 is believed to be the ROS that best fits the requirements for a second messenger, based on attributes, such as its relative stability and ability to traverse membranes through diffusion or channels [1, 31]. Previous studies have implicated H_2O_2 as a regulator of cellular migration [32–34] and demonstrated that FAK phosphorylation can be regulated by H_2O_2 in a dose dependent manner [16–19]. Interestingly, the effects on FAK phosphorylation were relatively modest and we observed that endogenous H_2O_2 shifts regulate migratory phenotype *via* redox-dependent changes in p130Cas phosphorylation. This scaffolding molecule of the FAK/Src signaling cascade has been implicated in regulating cell transformation and migration [35, 36], with significant increases in expression observed in breast, prostate and chronic myeloid leukemia [37–40]. p130Cas has also been found to regulate filopodia formation [41] and 3D migration in a collagen matrix [42]. In that context, we observed a more enhanced inhibitory effect on invasion though matrigel compared to migration over a 2D surface when inhibiting p130Cas expression in 253J-BV cells (Fig. 4). While redox-dependent shifts in both FAK and Src phosphorylation were observed, the most striking difference was observed at the level of p130Cas^{Y165}.

Interestingly, Fonseca *et al.* reported that p130Cas phosphorylation was difficult to detect unless cells were pretreated with vanadate, highlighting the importance of phosphatases in regulating p130Cas phosphorylation [21]. It was previously shown that phosphorylation stabilizes p130Cas and results in decreased protein degradation [43]. This may explain the higher total levels of this protein observed in some of our experiments from cell lines displaying enhanced intracellular ROS levels. We are actively investigating whether this ROS dependent change in p130Cas phosphorylation enhances protein stability and are also not ruling out a potential redox component to the transcriptional regulation of p130Cas.

Oxidation of PTPs is increasingly being recognized as a molecular mechanism by which ROS act as second messengers. It is therefore not surprising that an enhanced redox environment, as observed in metastatic 253J-BV cells, is sufficient in mediating oxidation of PTPs involved in regulating pro-migratory signaling. We show that endogenous shifts in steady state H_2O_2 that accompanies acquisition of the metastatic phenotype enhance thiol oxidation and decreases total PTP activity. PTPN12, the primary PTP involved in p130Cas de-phosphorylation is important in regulating cellular migration and focal adhesion assembly, specifically by regulating the activation of Rac-1, and has previously been shown to be under regulation by oxidation [23, 44–47]. Further, subtle decreases in PTPN12 levels had a profound impact tumor cell migration and p130Cas signaling (Fig. 5C).

The ability of cancer cells to migrate from their primary to a secondary sited involves coordinating events that induce detachment, alter integrin engagement and allow migration through ECM. ROS through H_2O_2 regulate a multitude of cellular signaling cascades primarily due to their ability to reversibly oxidize thiolate anions of cysteine residues [1, 8]. Many of the redox-sensitive signals control distinct aspects of the migratory and invasive phenotype. Rhee and coworkers first identified the dual lipid phosphatase PTEN as reversibly sensitive to H_2O_2-dependent inactivation[48]. PTEN plays a critical role in modulating phosphoinositide distribution during directed migration [49] and its oxidation by mitochondrial-derived H_2O_2 drives both the angiogenic and migratory phenotype[24]. H_2O_2 generation has been shown to be targeted at focal complexes in lamellipodia and membrane ruffles through tethering NADPH oxidase family members via scaffolding proteins. This compartmentalized production of ROS is directed at tyrosine phosphatases that are enriched in these compartments [50, 51]. Our prior work indicates that lamellipodia are also enriched in mitochondria and provide an additional source for migratory ROS production. Indeed, recent work using a mitochondrial-targeted catalase construct developed in our laboratory[52] indicates that mitochondrial ROS generation contributes to VEGF-dependent endothelial cell migration [53]. We have also established that many of the key migratory signaling molecules that are engaged during endothelial cell migration also drive the invasiveness of metastatic bladder cancer cells. Thus, the increase in steady state H_2O_2 associated with acquisition of the metastatic phenotype likely drives phosphatase inactivation leading to activation of FAK, Rho-related small GTPase Rac1 and MAP kinase signaling. However, a key difference is that these redox-driven signals are constitutively active in metastatic bladder cancer. It is our hypothesis that oxidants converge to drive the invasiveness of bladder tumors thus opening a therapeutic window to limit metastatic disease progression using targeted-antioxidant based therapeutics.

These studies indicate that the ability to endure chronic oxidative stress is a feature acquired by metastatic cancer cells. Current neoadjuvant therapies for metastatic bladder disease display similar therapeutic efficacy and despite initial high response rates these treatments are not curative. Our preliminary work has identified imbalances in the redox-milieu as contributing to the metastatic phenotype. It is likely that oxidizing species impinge on a number of molecular targets that as a whole serve to engage metastatic disease progression.

Thus, antioxidants may prove beneficial in limiting disease relapse when appropriately administered.

Supplementary Material

Refer to Web version on PubMed Central for supplementary material.

Acknowledgments

Our thanks go to Ms. Erin Moore, Mr. Ryan Clark, Ms. Usawadee Dier and Dr. Hanqing Ye for their technical assistance. We thank Dr. Colin P.N. Dinney (MD Anderson Cancer Center) for providing 253J and 253J-BV cell lines. This work was supported by NIH award numbers F32CA134165 & K99/R00CA143229 to NH and R01AG031067 to JAM.

Nonstandard Abbreviations

5-IAF	5-iodoacetamine fluorosceine
CAT	Catalase
ECM	extracellular matrix
FAK	Focal Adhesion Kinase
H_2O_2	Hydrogen Peroxide
IAA	iodoacetic acid
lacZ	beta galactosidase control vector
MMP	Matrix Metalloproteinase
NAC	N-acetyl-L-cysteine
NEM	N-ethylmaleimide
Nox	NADPH oxidase
p130Cas	Crk-associated substrate
pNPP	para-nitrophenol phosphate
PTEN	phosphatase and tensin homolog
PTP	protein tyrosine phosphatase
ROS	Reactive Oxygen Species
Sod2	Manganese superoxide dismutase
VEGF	Vascular Endothelial Growth Factor

References

1. Forman HJ, Maiorino M, Ursini F. Signaling functions of reactive oxygen species. Biochemistry. 2010; 49(5):835–42. [PubMed: 20050630]
2. Hamanaka RB, Chandel NS. Mitochondrial reactive oxygen species regulate cellular signaling and dictate biological outcomes. Trends Biochem Sci. 2010; 35(9):505–13. [PubMed: 20430626]
3. Szatrowski TP, Nathan CF. Production of large amounts of hydrogen peroxide by human tumor cells. Cancer Res. 1991; 51(3):794–8. [PubMed: 1846317]
4. Nishikawa M. Reactive oxygen species in tumor metastasis. Cancer Lett. 2008; 266(1):53–9. [PubMed: 18362051]

5. Hempel N, Carrico PM, Melendez JA. Manganese superoxide dismutase (Sod2) and redox-control of signaling events that drive metastasis. Anticancer Agents Med Chem. 2011; 11(2):191–201. [PubMed: 21434856]
6. Pani G, Galeotti T, Chiarugi P. Metastasis: cancer cell's escape from oxidative stress. Cancer Metastasis Rev. 2010; 29(2):351–78. [PubMed: 20386957]
7. Ishikawa K, et al. ROS-generating mitochondrial DNA mutations can regulate tumor cell metastasis. Science. 2008; 320(5876):661–4. [PubMed: 18388260]
8. Weinberg F, Chandel NS. Reactive oxygen species-dependent signaling regulates cancer. Cell Mol Life Sci. 2009; 66(23):3663–73. [PubMed: 19629388]
9. Dinney CP, et al. Isolation and characterization of metastatic variants from human transitional cell carcinoma passaged by orthotopic implantation in athymic nude mice. J Urol. 1995; 154(4):1532–8. [PubMed: 7658585]
10. Hempel N, et al. Altered redox status accompanies progression to metastatic human bladder cancer. Free Radic Biol Med. 2009; 46(1):42–50. [PubMed: 18930813]
11. Nelson KK, et al. Elevated sod2 activity augments matrix metalloproteinase expression: evidence for the involvement of endogenous hydrogen peroxide in regulating metastasis. Clin Cancer Res. 2003; 9(1):424–32. [PubMed: 12538496]
12. Connor KM, et al. Manganese superoxide dismutase enhances the invasive and migratory activity of tumor cells. Cancer Res. 2007; 67(21):10260–7. [PubMed: 17974967]
13. Zhao Y, et al. The lysyl oxidase pro-peptide attenuates fibronectin-mediated activation of focal adhesion kinase and p130Cas in breast cancer cells. J Biol Chem. 2009; 284(3):1385–93. [PubMed: 19029090]
14. Yang Y, Song Y, Loscalzo J. Regulation of the protein disulfide proteome by mitochondria in mammalian cells. Proc Natl Acad Sci U S A. 2007; 104(26):10813–7. [PubMed: 17581874]
15. Streit S, et al. PTP-PEST phosphatase variations in human cancer. Cancer Genet Cytogenet. 2006; 170(1):48–53. [PubMed: 16965954]
16. Basuroy S, et al. Hydrogen peroxide activates focal adhesion kinase and c-Src by a phosphatidylinositol 3 kinase-dependent mechanism and promotes cell migration in Caco-2 cell monolayers. Am J Physiol Gastrointest Liver Physiol. 2010; 299(1):G186–95. [PubMed: 20378826]
17. Chiarugi P, et al. Reactive oxygen species as essential mediators of cell adhesion: the oxidative inhibition of a FAK tyrosine phosphatase is required for cell adhesion. J Cell Biol. 2003; 161(5): 933–44. [PubMed: 12796479]
18. Natarajan V, et al. Reactive oxygen species signaling through regulation of protein tyrosine phosphorylation in endothelial cells. Environ Health Perspect. 1998; 106(Suppl 5):1205–12. [PubMed: 9788899]
19. Vepa S, et al. Hydrogen peroxide stimulates tyrosine phosphorylation of focal adhesion kinase in vascular endothelial cells. Am J Physiol. 1999; 277(1 Pt 1):L150–8. [PubMed: 10409242]
20. Sakai R, et al. A novel signaling molecule, p130, forms stable complexes in vivo with v-Crk and v-Src in a tyrosine phosphorylation-dependent manner. EMBO J. 1994; 13(16):3748–56. [PubMed: 8070403]
21. Fonseca PM, et al. Regulation and localization of CAS substrate domain tyrosine phosphorylation. Cell Signal. 2004; 16(5):621–9. [PubMed: 14751547]
22. Tonks NK. Redox redux: revisiting PTPs and the control of cell signaling. Cell. 2005; 121(5):667–70. [PubMed: 15935753]
23. Garton AJ, Flint AJ, Tonks NK. Identification of p130(cas) as a substrate for the cytosolic protein tyrosine phosphatase PTP-PEST. Mol Cell Biol. 1996; 16(11):6408–18. [PubMed: 8887669]
24. Connor KM, et al. Mitochondrial H2O2 Regulates the Angiogenic Phenotype via PTEN Oxidation. J Biol Chem. 2005; 280(17):16916–16924. [PubMed: 15701646]
25. Huang L, et al. Identification of a gene-expression signature for predicting lymph node metastasis in patients with early stage cervical carcinoma. Cancer. 2011
26. Malafa M, et al. MnSOD expression is increased in metastatic gastric cancer. J Surg Res. 2000; 88(2):130–4. [PubMed: 10644478]

27. Ye H, et al. Proteomic based identification of manganese superoxide dismutase 2 (SOD2) as a metastasis marker for oral squamous cell carcinoma. Cancer Genomics Proteomics. 2008; 5(2):85–94. [PubMed: 18460737]
28. Chan K, Kan YW. Nrf2 is essential for protection against acute pulmonary injury in mice. Proc Natl Acad Sci U S A. 1999; 96(22):12731–6. [PubMed: 10535991]
29. Cho HY, et al. Role of NRF2 in protection against hyperoxic lung injury in mice. Am J Respir Cell Mol Biol. 2002; 26(2):175–82. [PubMed: 11804867]
30. Taylor RC, et al. Network inference algorithms elucidate Nrf2 regulation of mouse lung oxidative stress. PLoS Comput Biol. 2008; 4(8):e1000166. [PubMed: 18769717]
31. Miller EW, Dickinson BC, Chang CJ. Aquaporin-3 mediates hydrogen peroxide uptake to regulate downstream intracellular signaling. Proceedings of the National Academy of Sciences. 2010; 107(36):15681–15686.
32. Zhao Y, Davis HW. Hydrogen peroxide-induced cytoskeletal rearrangement in cultured pulmonary endothelial cells. J Cell Physiol. 1998; 174(3):370–9. [PubMed: 9462699]
33. Moldovan L, et al. Reactive oxygen species in vascular endothelial cell motility. Roles of NAD(P)H oxidase and Rac1. Cardiovasc Res. 2006; 71(2):236–46. [PubMed: 16782079]
34. Roy S, et al. Dermal wound healing is subject to redox control. Mol Ther. 2006; 13(1):211–20. [PubMed: 16126008]
35. Cabodi S, et al. Integrin signalling adaptors: not only figurants in the cancer story. Nat Rev Cancer. 2010; 10(12):858–70. [PubMed: 21102636]
36. Defilippi P, Di Stefano P, Cabodi S. p130Cas: a versatile scaffold in signaling networks. Trends Cell Biol. 2006; 16(5):257–63. [PubMed: 16581250]
37. Cabodi S, et al. p130Cas as a new regulator of mammary epithelial cell proliferation, survival, and HER2-neu oncogene-dependent breast tumorigenesis. Cancer Res. 2006; 66(9):4672–80. [PubMed: 16651418]
38. Celhay O, et al. Expression of estrogen related proteins in hormone refractory prostate cancer: association with tumor progression. J Urol. 2010; 184(5):2172–8. [PubMed: 20850840]
39. Salgia R, et al. p130CAS forms a signaling complex with the adapter protein CRKL in hematopoietic cells transformed by the BCR/ABL oncogene. J Biol Chem. 1996; 271(41):25198–203. [PubMed: 8810278]
40. van der Flier S, et al. Immunohistochemical study of the BCAR1/p130Cas protein in non-malignant and malignant human breast tissue. Int J Biol Markers. 2001; 16(3):172–8. [PubMed: 11605729]
41. Gustavsson A, Yuan M, Fallman M. Temporal dissection of beta1-integrin signaling indicates a role for p130Cas-Crk in filopodia formation. J Biol Chem. 2004; 279(22):22893–901. [PubMed: 15044442]
42. Fraley SI, et al. A distinctive role for focal adhesion proteins in three-dimensional cell motility. Nat Cell Biol. 2010; 12(6):598–604. [PubMed: 20473295]
43. Weng LP, Wang X, Yu Q. Transmembrane tyrosine phosphatase LAR induces apoptosis by dephosphorylating and destabilizing p130Cas. Genes Cells. 1999; 4(3):185–96. [PubMed: 10320483]
44. Angers-Loustau A, et al. Protein tyrosine phosphatase-PEST regulates focal adhesion disassembly, migration, and cytokinesis in fibroblasts. J Cell Biol. 1999; 144(5):1019–31. [PubMed: 10085298]
45. Sastry SK, et al. PTP-PEST controls motility through regulation of Rac1. J Cell Sci. 2002; 115(Pt 22):4305–16. [PubMed: 12376562]
46. Diaz B, et al. Tks5-dependent, nox-mediated generation of reactive oxygen species is necessary for invadopodia formation. Sci Signal. 2009; 2(88):ra53. [PubMed: 19755709]
47. Ceacareanu AC, et al. Nitric oxide attenuates IGF-I-induced aortic smooth muscle cell motility by decreasing Rac1 activity: essential role of PTP-PEST and p130cas. Am J Physiol Cell Physiol. 2006; 290(4):C1263–70. [PubMed: 16354758]
48. Lee SR, et al. Reversible inactivation of the tumor suppressor PTEN by H2O2. J Biol Chem. 2002; 277(23):20336–20342. [PubMed: 11916965]

49. Franca-Koh J, Kamimura Y, Devreotes PN. Leading-edge research: PtdIns(3,4,5)P3 and directed migration. Nat Cell Biol. 2007; 9(1):15–17. [PubMed: 17199126]

50. Wu RF, et al. Subcellular targeting of oxidants during endothelial cell migration. The Journal of Cell Biology. 2005; 171(5):893–904. [PubMed: 16330715]

51. Ushio-Fukai M. Compartmentalization of redox signaling through NADPH oxidase-derived ROS. Antioxidants & Redox Signaling. 2009; 11(6):1289–99. [PubMed: 18999986]

52. Rodriguez AM, et al. Mitochondrial or cytosolic catalase reverses the MnSOD-dependent inhibition of proliferation by enhancing respiratory chain activity, net ATP production, and decreasing the steady state levels of H(2)O(2). Free Radic Biol Med. 2000; 29(9):801–813. [PubMed: 11063906]

53. Wang Y, et al. Regulation of VEGF Induced Endothelial Cell Migration by Mitochondrial Reactive Oxygen Species. American journal of physiology. Cell physiology. 2011

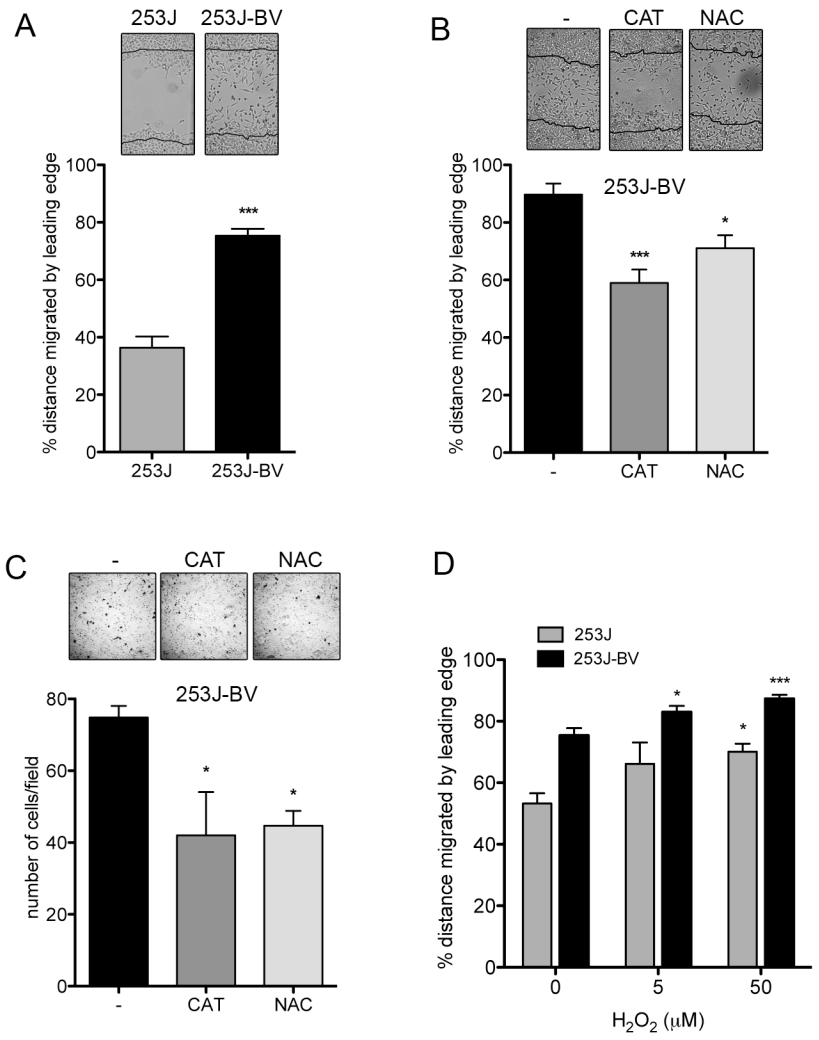

FIGURE 1.

Intracellular redox status regulates migration and invasion of metastatic bladder cancer cells. (A) Metastatic 253J-BV cells migrate at a faster rate than 253J cells in a wound healing assay. Wound edge at time 0 is marked on the image and % distance migrated by leading edge after 16 hrs quantified (n=8; mean +/− SEM, t-test, ***p<0.0001). (B) Antioxidants CAT (500U/ml) and NAC (2mM) inhibit migration of 253J-BV cells. Cells were pre-treated for 18 hours in complete media. Wound healing was carried out in 0% serum DMEM containing the same antioxidant concentrations for 24 hrs (n=5; mean +/− SEM, One-way ANOVA, *p<0.05, ***p<0.001). (C) CAT (500U/ml) and NAC (2mM) inhibit 253J-BV invasion. Cells were pre-treated for 18 hours with antioxidants in complete media and assayed for invasion through matrigel coated transwell chambers towards the chemo-attractant (10% serum). Cells on the bottom surface of the chamber were quantified (n=3; mean +/− SEM, One-way ANOVA, *p<0.05). (D) Sub-lethal levels of H_2O_2 enhance bladder cancer cell migration. 253J and 253J-BV cells were allowed to migrate for 21hrs (n=8; mean +/− SEM, One-way ANOVA, *p<0.05, ***p<0.001, compared to 0μM H_2O_2).

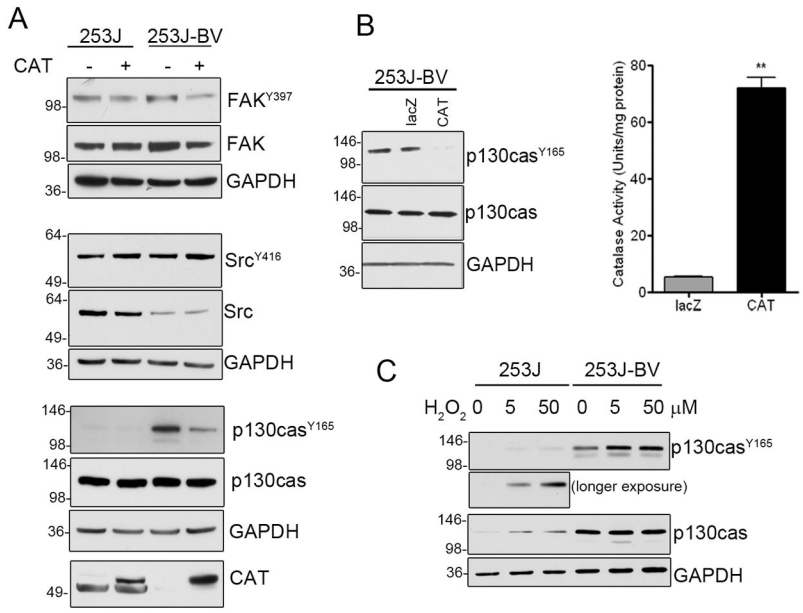

FIGURE 2.

Redox regulation of pro-metastatic signaling *via* p130Cas. (A) Cells were pretreated for 24hrs with recombinant CAT (500U/ml), followed by 18hr serum deprivation containing the same CAT treatment prior to cell lysis and immunoblotting with phospho-specific antibodies against Y397 FAK, Y416 Src an Y165 p130Cas (B) Phosphorylation of Y165 p130cas in 253J-BV cells is decreased following expression of CAT by adenoviral gene delivery (lac-Z = control). CAT activity was significantly enhanced following adenoviral gene delivery (n=3, mean +/− SEM, t-test, **p<0.01). (C) Y165 p130Cas phosphorylation increases following exogenous sub-lethal H_2O_2 treatment. Cells were treated with indicated doses for 16 hrs in serum free media.

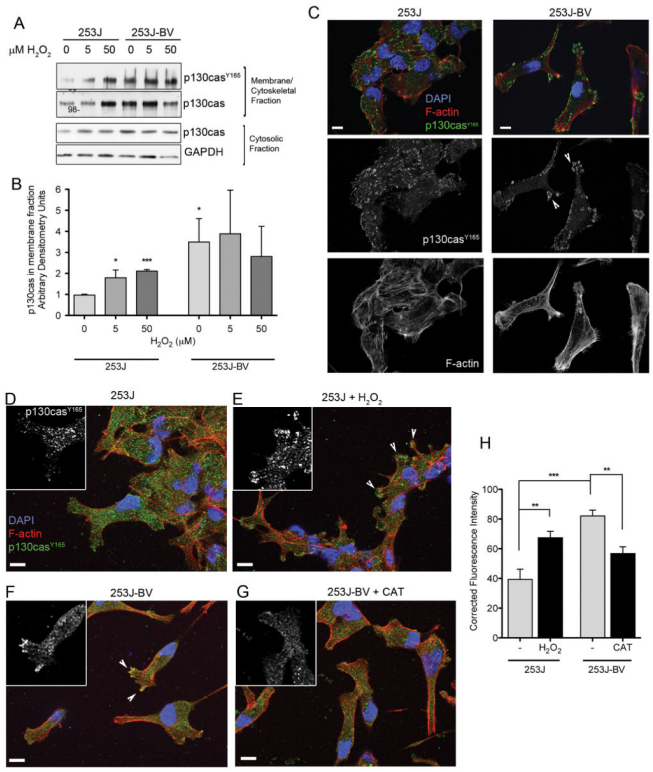

FIGURE 3.

Intracellular redox status regulates p130Cas cellular localization. (A) p130Cas is more abundant in the membrane/cytoskeletal fraction of 253J-BV cells than 253J cells. H_2O_2 treatment (10min) enhances p130Cas membrane recruitment as assessed by membrane / cytosol fractionation. (B) Quantification of p130Cas immunoreactive protein in membrane fractions normalized to GAPDH levels. (C) Immunofluorescent staining reveals enhanced membrane distribution of phospho p130Cas in metastatic 253-BV compared to 253J cells. Cells were fixed and stained for phospho-p130Cas Y165 (Alexa Fluor 488, green), Nucleus (Dapi, blue) and F-actin (Phalloidin-Texas Red). Following mounting, images were acquired using Zeiss AxioObserver.Z1 with AxioCamM3, Apotome (63x/1.25NA oil objective; Scale bar = 10 μm). (D–G) Phospho p130Cas localization at the leading edge is dependent on redox status of cells. 253J or 253J-BV cells were plated on coverslips, allowed to reach a confluent monolayer and monitored for migration following scratch wounding in serum free media, with or without 50μM H_2O_2 (253J, D & E) or 500U/ml CAT (253J-BV, F & G). After 6 hours, cells were fixed and immune-fluorescently labeled for Phospho p130Cas Y165 (Alexa Fluor 488, green), Nucleus (Dapi, blue) and F-actin (Phalloidin-Texas Red). White arrows point to examples of phospho-p130Cas positive protrusions. Images were taken of cells at the wound edge migrating into the direction of the opposing leading edge of cells (indicated by red arrows), using Zeiss AxioObserver.Z1 with AxioCamM3, Apotome (63x/1.25NA oil objective; Scale bar = 10 μm). (H) Quantification of the number of phospho p130Cas positive protrusions (6–10 images per treatment quantified, with a range of 5–20 protrusions per image; One-way ANOVA, **p<0.01, ***p<0.001).

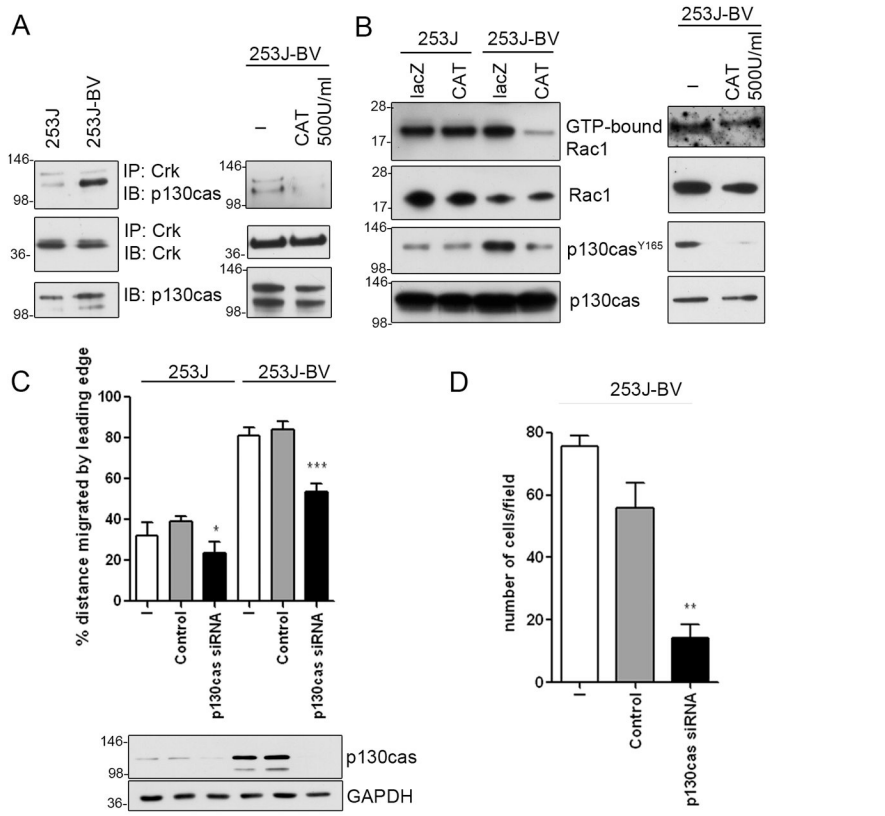

FIGURE 4.

p130Cas down-stream signaling is redox-dependent. (A) Intracellular redox status regulates Crk-p130Cas interaction. Cells were lysed using RIPA buffer, followed by immunoprecipitation (IP) with antibody against Crk and immunoblotting (IB) with indicated antibodies. CAT treatment (as in Fig. 2) abrogates association of Crk with p130Cas. (B) Rac1 activation in 253J-BV cells is decreased following CAT adenoviral delivery or exogenous CAT treatment. GTP-bound active Rac1 was isolated from cell lysates using PAK-1 binding domain conjugated agarose, as described in methods. Total Rac1, Phospho-p130Cas and total p130Cas levels were assessed by IB of input. (C) p130Cas knock-down significantly abrogates 253J-BV migration in a wound healing assay. Cells were mock transfected (−), with siRNA construct against p130Cas or scramble control prior to wound healing assay (n=7; mean +/− SEM, t-test, *p<0.05, ***p<0.0001, compared to scramble control). Immunoblot for p130Cas shows efficiency of p130Cas protein knock-down. (D) siRNA p130Cas knock-down decreases invasive properties of 253J-BV cells through matrigel. Cells invaded through to the bottom surface of the transwell chamber were quantified (n=3; mean +/− SEM, t-test, **p<0.01, compared to scramble control).

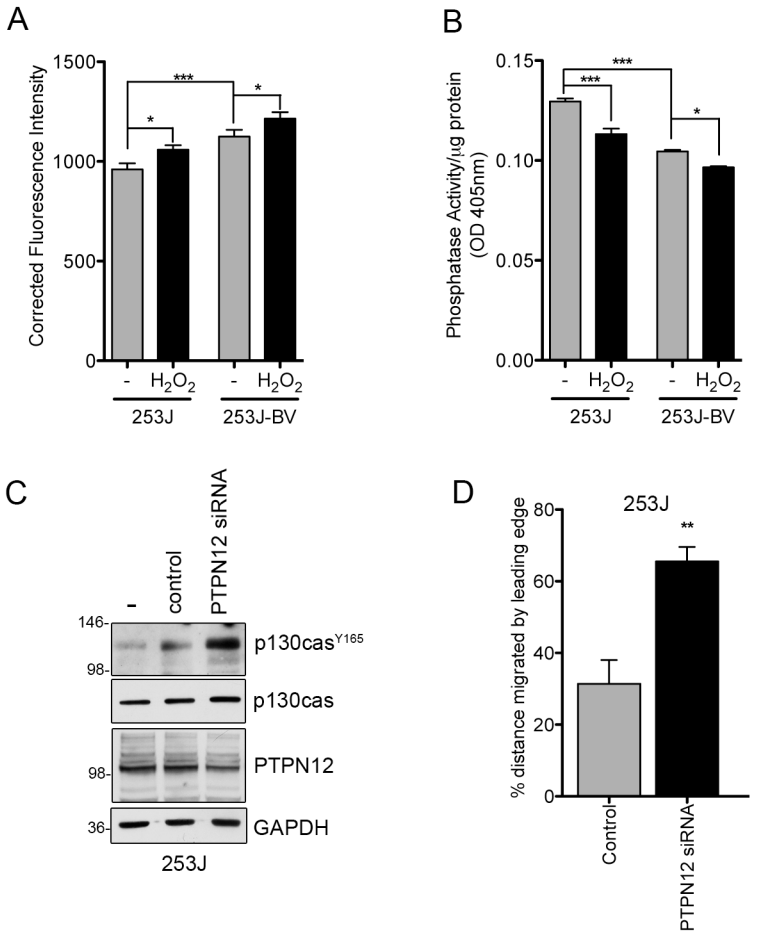

FIGURE 5.

Enhanced intracellular redox status leads to increase in PTPN12 oxidation. (A) Total protein disulfide status of cells with or without 50μM H_2O_2 (10 min) was assessed using reverse *in situ* 5- iodoacetamine fluorosceine (5-IAF) labeling as outlined in methods. All reduced thiol residues were alkylated using non-labeled IAA. The remaining disulfides were reduced with DTT and acetylated using 5-IAF. Significant increases in *in situ* 5-IAF labeling were observed in 253J-BV cells compared to 253J cells using an Olympus Fluoview1000 Confocal Microscope. Average intensity units per cell were measured following background correction (n=30, mean +/− SEM, t-test, *p<0.05, ***p<0.001). (B) Total phosphatase activity is decreased in 253J-BV cells. Cells were treated with or without 50μM H_2O_2 for 10 min in serum free media and the ability of cell lysates to dephosphorylate *p*-nitrophenol–phosphate was assessed colorimetrically. (C) Knock-down of PTPN12 in 253J cells increases p130Cas Y165 phosphorylation. Cells were mock transfected (−), with siRNA construct against PTPN12 or scramble control, and cell lysates subjected to immunoblotting with the indicated antibodies. (D) PTPN12 knock-down significantly enhances migration of 253J cells in wound healing assays. Cells were transfected as in (D), monitored for migration for 17 hrs and percent distance migrated by leading edge quantified (n=4; mean +/− SEM, t-test, *p<0.05, **p<0.01, compared to scramble control).